Epitaxial growth of $Si_{1-x}Ge_x$ on Si(100)2 × 1: A molecular-dynamics study

Stéphane Ethier and Laurent J. Lewis[a)]
Département de physique et Groupe de recherche en physique et technologie des couches minces, Université de Montréal, Case postale 6128, succursale A, Montréal, Québec H3C 3J7, Canada

(Received 31 May 1991; accepted 23 June 1992)

We use molecular-dynamics simulations to study the growth of pure Si, $Si_{0.5}Ge_{0.5}$, and pure Ge on the 2 × 1 reconstructed surface of Si(100) in a way appropriate to the fabrication of thin films by the method of molecular-beam epitaxy (MBE), namely sequential deposition of energetic atoms. The atoms interact with one another via effective potentials of the Stillinger–Weber form, with parameters adjusted such as to describe all possible types of triplet interactions. Motivated by numerous experimental studies of MBE-grown films, we investigate in particular the structure of the deposits as a function of substrate temperature. We find in all three cases that at low substrate temperatures, poorly ordered structures form, while at high substrate temperatures, epitaxial growth takes place. The presence of Ge limits the number of crystalline overlayers that form, even though it appears to favor a more-ordered structure in the *initial* stages of growth. For pure Ge epitaxy, in particular, only the first three layers are crystalline, after which growth appears to proceed by the formation of islands, reminiscent of the Stranski–Krastanow growth scheme, and in qualitative agreement with recent experimental and theoretical work. In all samples, annealing improves the quality of the films—at least when grown at sufficiently high substrate temperatures. The interdiffusion of the species at the substrate-deposit interface is also examined.

I. INTRODUCTION

There is a great deal of interest in heterostructures and superlattices, in particular Si/Ge, since their electrical and optical properties put them on the front line for the fabrication of optoelectronic devices such as photodiodes, solid-state lasers, ultrafast photodetectors, etc.[1] However, the development of quality material with tailor-made characteristics greatly depends on film-growth techniques.[2] Among these, molecular-beam epitaxy (MBE) is one of the most extensively used, because of its ability to grow high-quality films; in particular, it leads to sharp and uniform interfaces, thus making it appropriate for the fabrication of superlattices.[3]

The dynamical and kinetic processes that take place during fabrication are very complex and, unfortunately, not very well understood. The properties of $Si_{1-x}Ge_x$ ($0 \leq x \leq 1$), and in particular its epitaxy on Si or Ge, have been the object of innumerable experimental[4–12] and theoretical studies.[13–16] A powerful tool for probing the microstructures of materials is molecular dynamics (MD), and the technique has been applied to the study of a variety of problems in materials science.[17] The MBE process has itself been the object of several such studies,[18–26] but was in all those cases restricted to the problem of homoepitaxy of Si on Si. The heteroepitaxy of $Si_{1-x}Ge_x$ on Si has, to our knowledge, never been investigated in this way, though mismatched systems have been examined.[27]

Here we do so by studying the growth of the $Si_{0.5}$-$Ge_{0.5}$ alloy[28] and that of pure Ge on the reconstructed (100) surface of silicon.[29] Thus we use MD and sequential deposition of atoms to simulate MBE growth. As a check of the validity of the model, we first look at the growth of pure Si on Si(100). We find that low-temperature deposition (150 K) produces disordered layers that do not reorder perfectly even under prolonged high-temperature annealing. At high substrate temperatures (800–1000 K), on the other hand, we observe good epitaxial growth, without recourse to annealing, though annealing does improve the crystallinity of the films. Interestingly, the presence of Ge atoms, at least for the $x = 0.5$ system grown at high temperature, also appears to improve the situation, though in this case interfacial strains seem to prevent the formation of thick epitaxial layers. For pure Ge, for instance, the growth is epitaxial only for the first two or three monolayers, in agreement with recent experimental[4,7,8] and theoretical[14] work, and then proceeds by the formation of islands that grow in height, in a way reminiscent of the growth mode proposed by Stranski and Krastanow.[30] Very high-temperature (1500 K and more) growth, finally, leads to serious deterioration of the films.

Our paper is organized as follows: First, we present our model, namely the initial (unreconstructed) Si(100)

[a)]Author to whom correspondence should be addressed.

 © 1992 Materials Research Society

substrate, the potentials, and the method used for depositing the atoms. Results for all three systems are presented in Sec. III, where we describe in particular the effect of varying the substrate temperature, and that of high-temperature annealing. A summary and conclusions are given in Sec. IV.

II. MODEL

A. Substrate and deposition

The atomic model we employ is similar to that used by other authors,[19–26] and is schematically depicted in Fig. 1(a). Here, the system is shown after approximately one layer has been deposited. The substrate of pure crystalline silicon is oriented along the [100] direction and consists of eight square layers of 32 atoms each. The bottom two layers are held fixed in order to accommodate the free boundary conditions along the direction perpendicular to the surface, while the usual periodic boundary conditions are imposed in the other two directions so as to mimic an infinite system; thus, an atom that leaves the system by one of the four lateral faces automatically re-enters from the opposite face.

In order to simulate the incident molecular beam, atoms are created at random in a plane above the surface, as depicted in Fig. 1(a). The distance from this plane to the surface of the sample is at all times required to be larger than the range of interaction of the potential (see Sec. II. B). The beam was chosen to be normally incident on the surface. Other angles are, of course, possible. For instance, by choosing a grazing angle, it is possible to investigate surface channeling, as was done, for instance, by Dodson on the (111) surface of Si.[23] Since our main interest is in the growth under conditions appropriate to MBE, the angle was not varied.

The energy of the molecular beam was taken to be 0.38 eV, which is typical of MBE experiments.[3] This corresponds to a temperature substantially higher than

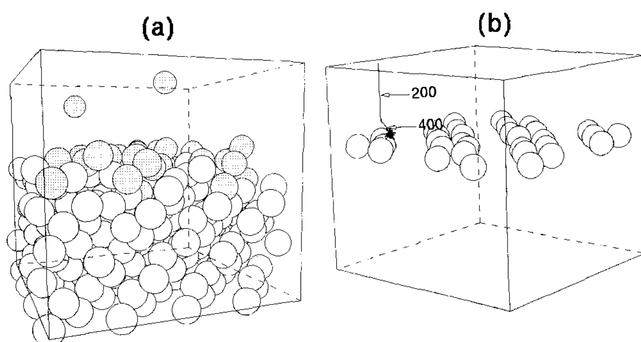

FIG. 1. (a) Model for simulating the deposition process. White circles: original substrate; grey circles: deposited atoms. (b) Trajectory of a typical atom during deposition on the substrate at 800 K. The numbers indicate the time, in fs, since its creation.

the fusion temperature of Si. Other authors have used similar values.[19] The proper beam temperature and other parameters should be such that energy (both kinetic and binding) brought onto the surface by the impinging atoms does not accumulate. The excess energy is evacuated by coupling the system—substrate plus deposited layers—to an external heat bath. This is achieved by rescaling the velocities of the atoms in a number of appropriately chosen "cooling layers" at every time step, a number that varies with time. Luedtke and Landman[22] have shown that one layer is insufficient for this purpose—the system simply melts. We found it convenient and efficient to use all but the topmost two mobile layers. The latter are thus free from any constraints. This procedure ensures that cooling interferes minimally with the growth process, but still efficiently evacuates the excess energy.

It should be noted that, because the bottom two layers are fixed (i.e., have zero temperature) while the surface layers are heated up at a constant rate, a temperature gradient will develop in the system. If cooling is efficient, this gradient will rapidly attain an essentially steady state. Its amplitude, of course, depends on the incident particle temperature, as well as the rate at which they are being deposited. Thus, we expect the temperature of the deposited layers to be some average, appropriately weighted by the deposition rate, of the beam and substrate temperatures. At very high deposition rates, the surface melts, while at very low rates, the deposited layers are in perfect equilibrium with the substrate. The effect of varying the substrate temperature will be described in detail in Sec. III.

In the present simulations, the parameters of the model were determined self-consistently by requiring that the surface reaches a fully relaxed state in the time comprised between the arrival of two successive atoms. Thus, for low substrate temperatures (T_s = 150 K), we used a deposition rate of 1 atom every 0.5 ps, while for intermediate and high temperatures (T_s = 500 to 1800 K) a rate of 1 atom every 0.2 ps was found to be adequate. Though these deposition rates are unrealistically large (in comparison with experimental situations), such difficulties are common to all MD studies. Our procedure nevertheless ensures that the surface remains in satisfactory equilibrium with the substrate. Figure 1(b) shows the first 500 fs of the trajectory of a Si atom impinging on the Si(100) surface. In this case, the substrate temperature T_s = 800 K. Clearly, the atom and the surface rapidly reach equilibrium; i.e., the incident atom undergoes very little surface diffusion at this temperature.

In the growth experiments to be discussed in Sec. III, a total of 160 atoms were in each case deposited, corresponding to five full monolayers in the present model. In order to improve on the quality of the films, as we will see, each sample was subjected, following deposition,

to a prolonged heat treatment, i.e., was taken to a temperature of 1500 K (which is somewhat below the melting temperature of the Stillinger–Weber model of Si,[31] namely 1691 K)[32] for a period of 75–100 000 MD time steps (=75–100 ps in real time).

B. Interaction potentials

Many empirical potentials have been developed to describe the structural properties of silicon.[31,33–35] Among them, the one proposed by Stillinger and Weber,[31] has certainly been the most extensively used. It has been shown to give a reasonable account of various thermodynamic properties.[36] We also chose this model in our study, with parameters for the mixed Si–Ge interactions adjusted as detailed below. Though they would be ideal, *ab initio* molecular-dynamics calculations are presently not practical for such large simulations.[37] It should be said that an empirical potential for $Si_{1-x}Ge_x$ solid solutions was developed by Ito, Khor, and Das Sarma.[38] However, the analytical complexity of this potential renders it impractical for large-scale molecular-dynamics simulations. Very recently, Khor and Das Sarma have proposed an improved version of this model.[39]

The Stillinger–Weber potential is written as a sum of two- and three-body interactions,

$$V_{\mathrm{tot}} = \sum_{i,j(i<j)} v_2(i,j) + \sum_{i,j,k(i<j<k)} v_3(i,j,k), \quad (1)$$

with

$$v_2(r_{ij}) = \epsilon f_2(r_{ij}/\sigma), \quad (2)$$

and

$$v_3(\mathbf{r}_i, \mathbf{r}_j, \mathbf{r}_k) = \epsilon f_3(\mathbf{r}_i/\sigma, \mathbf{r}_j/\sigma, \mathbf{r}_k/\sigma). \quad (3)$$

The parameters ϵ and σ fix the energy and length scales, respectively. The two-body potential function is

$$f_2(r) = \begin{cases} A(Br^{-p} - r^{-q}) \exp[(r-a)^{-1}] & r < a \\ 0 & r \geqslant a \end{cases}, \quad (4)$$

where A, B, p, q, and a are all positive constants (full details of the potential can be found in the original reference).[31] For the three-body function, we have:

$$f_3(\mathbf{r}_i, \mathbf{r}_j, \mathbf{r}_k) = h(r_{ij}, r_{ik}, \theta_i) + h(r_{ji}, r_{jk}, \theta_j) + h(r_{ki}, r_{kj}, \theta_k), \quad (5)$$

with

$$h(r_{ij}, r_{ik}, \theta_i) = \lambda \exp \gamma[(r_{ij} - a)^{-1} + (r_{ik} - a)^{-1}] \times (\cos\theta_i + 1/3)^2, \quad (6)$$

where θ_i is the angle between $\mathbf{r}_{ij} = \mathbf{r}_j - \mathbf{r}_i$ and $\mathbf{r}_{ik} = \mathbf{r}_k - \mathbf{r}_i$, for the triplet of atoms (i, j, k). γ and λ are also positive quantities.

In order to describe all the interactions between any combination of three atoms, each being either Si or Ge, six sets of parameters are needed. The parameters for the Stillinger–Weber potential have unfortunately been determined only for pure Si[31] and pure Ge.[40] In the case of Ge, the parameters were obtained rather loosely: indeed, Ding and Andersen simply retained the Stillinger–Weber parameters for Si, except for ϵ, σ, and λ, where the latter is a measure of the strength of the three-body interaction. We adopted the same philosophy here, and allowed only the above three parameters to vary in the case of mixed interactions. Equations (2) to (6) must therefore be generalized to:

$$v_2(r_{ij}) = \begin{cases} \epsilon_{ij} A\left(B\left(\frac{r_{ij}}{\sigma_{ij}}\right)^{-p} - \left(\frac{r_{ij}}{\sigma_{ij}}\right)^{-q}\right) \exp\left[\left(\frac{r_{ij}}{\sigma_{ij}} - a\right)^{-1}\right] & \frac{r_{ij}}{\sigma_{ij}} < a \\ 0 & \frac{r_{ij}}{\sigma_{ij}} \geq a \end{cases}, \quad (7)$$

$$v_3(\mathbf{r}_i, \mathbf{r}_j, \mathbf{r}_k) = \varepsilon_{ijk} h\left(\frac{r_{ij}}{\sigma_{ij}}, \frac{r_{ik}}{\sigma_{ik}}, \theta_i\right) + \epsilon_{jik} h\left(\frac{r_{ji}}{\sigma_{ji}}, \frac{r_{jk}}{\sigma_{jk}}, \theta_j\right) + \epsilon_{kij} h\left(\frac{r_{ki}}{\sigma_{ki}}, \frac{r_{kj}}{\sigma_{kj}}, \theta_k\right), \quad (8)$$

and

$$h\left(\frac{r_{ij}}{\sigma_{ij}}, \frac{r_{ik}}{\sigma_{ik}}, \theta_i\right) = \lambda_{ijk} \exp \gamma \times \left[\left(\frac{r_{ij}}{\sigma_{ij}} - a\right)^{-1} + \left(\frac{r_{ik}}{\sigma_{ik}} - a\right)^{-1}\right]\left(\cos\theta_i + \frac{1}{3}\right)^2. \quad (9)$$

The parameters for the mixed interactions were determined using standard combination rules,[41] i.e., arithmetic mean for distances, and geometric mean for energies. Thus, for cross terms, the length scale is given by $\sigma_{ij} = (\sigma_i + \sigma_j)/2$ (which agrees extremely well with experimental data),[42] while the energy scales for the two- and three-body parts of the potential become $\epsilon_{ij} = \sqrt{\epsilon_i \epsilon_j}$ and $\epsilon_{ijk} = \sqrt{\epsilon_{ij} \epsilon_{ik}}$, respectively. The three-body energy parameter, λ, finally, is replaced by $\lambda_{ijk} = \sqrt{\lambda_{ij} \lambda_{ik}}$ where $\lambda_{ij} = \sqrt{\lambda_i \lambda_j}$. In the above, i is the atom on which we calculate the force and j, k are its neighbors. It should be noted that both three-body parameters are invariant under a permutation of j and k. With the above mixing rules, all six sets of parameters can be inferred from the knowledge of only two of them, namely those for pure Si and pure Ge. They are given explicitly in Table I.

From a practical viewpoint, we note that the above choice still allows use of the Biswas–Hamann decomposition scheme,[35] which rewrites the angular part of the three-body potential as a sum of two-body contributions. This is extremely advantageous computationally, since

TABLE I. Parameters of the potentials used in the present calculations, Eqs. (7)–(9). For three-body contributions, the index i denotes the atom located at the vertex (i.e., the one on which the force is to be calculated).

Constants		σ_{ij} (nm)		λ_{ijk}		ϵ_{ijk} (10^{-19} J)	
A	7.050	Si–Si	0.2095	Si–Si–Si	21.0	Si–Si–Si	3.472
B	0.6022	Si–Ge	0.2138	Si–Si–Ge	23.1	Si–Si–Ge	3.371
p	4	Ge–Ge	0.2181	Si–Ge–Ge	25.5	Si–Ge–Ge	3.273
q	0			Ge–Si–Si	25.5	Ge–Si–Si	3.273
a	1.8			Ge–Si–Ge	28.1	Ge–Si–Ge	3.178
γ	1.2			Ge–Ge–Ge	31.0	Ge–Ge–Ge	3.085

the number of operations at each time step is then reduced from order NZ^2 to NZ, where N is the total number of atoms, and Z is the average number of neighbors within the range of interaction of the potential (here, $N = 256$–416, and $Z = 20$).

The present MD simulations were carried out at constant volume. The equations of motion were integrated using a fifth order Gear predictor-corrector algorithm,[41,43] with a time step of 1 fs, which resulted in energy conservation of typically 1 part in 10^6 (for a review of MD techniques, see, for instance, Refs. 41 and 44).

III. RESULTS AND DISCUSSION

A. 2 × 1 reconstruction of Si(100)

In order to prepare the substrate for deposition, we first let it attain thermodynamic equilibrium by performing an undisturbed MD relaxation. Like all authors who used the Stillinger–Weber potential to simulate the free (100) surface of silicon,[18,22,25] we observe the 2 × 1 reconstruction at all temperatures. An example of the effect of relaxing the free surface is presented in Fig. 2: the reconstruction takes place rapidly, typically within 0.2–0.5 ps, especially at high temperatures. This gives us further justification for our choice of rate of deposition, discussed in Sec. II. A.

We remark here that reconstruction is a dynamic process, and in particular it is reversible. Thus, we expect the surface to "deconstruct", i.e., to return to its bulk configuration after two full layers have been deposited (corresponding to the range of three-body correlations in our model). All deposits were therefore grown on the reconstructed surface. A detailed discussion of the results follows.

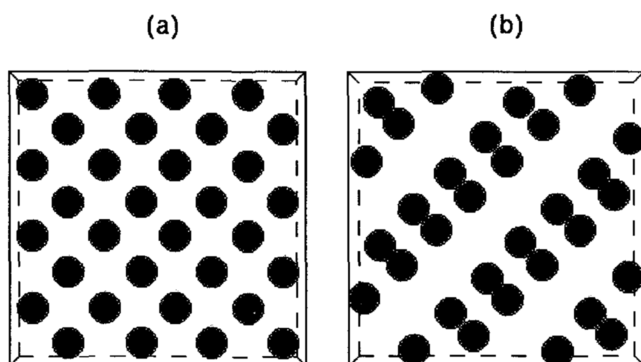

FIG. 2. 2 × 1 reconstruction of the (100) surface of Si: (a) before and (b) after relaxation.

B. Si on Si(100)2 × 1

In order to test the validity of our model, we first discuss the homoepitaxy of Si on Si(100). At low substrate temperatures, 150 K and below, we find all deposited layers to be disordered. Figure 3(a) shows the results of an experiment at $T_s = 150$ K, immediately after deposition of the last atom. (In Fig. 3 and subsequent, a "layer" is defined as a slice of thickness $a/4$ through space in a direction perpendicular to the surface, where a is the lattice parameter. For crystalline systems, layers are well defined, whereas for disordered systems, the concept is merely used for convenience. For future reference, one should keep in mind that the layer labeled #8 corresponds to the initial top layer of the substrate.) Clearly, at this temperature, the system exhibits considerable disorder, and there is very little sign of epitaxy. Nevertheless, the initial surface has almost completely recovered its bulk configuration, while reconstruction takes place elsewhere. There is in fact a strong correlation between the formation of dimers and the location of voids in subsequent layers.

We now anneal the system as discussed in Sec. II. A. The result of this treatment is shown in Fig. 3(b): dramatic improvement over the preannealed state takes place. The initial top layer (#8) has completely reordered, and the deposited film is epitaxial for its most part. Reconstruction is clearly visible in the last two layers, #13 and 14; we observe also that dimerization takes place at perpendicular directions in successive layers, as indeed observed experimentally.[45] It is interesting to note that several atoms from layer #8 (black circles) have been ejected from their original positions and replaced by incoming particles (white circles). Upon comparing Figs. 3(a) and 3(b), it is clear that such processes take place during the deposition, i.e., *not* during the anneal cycle.

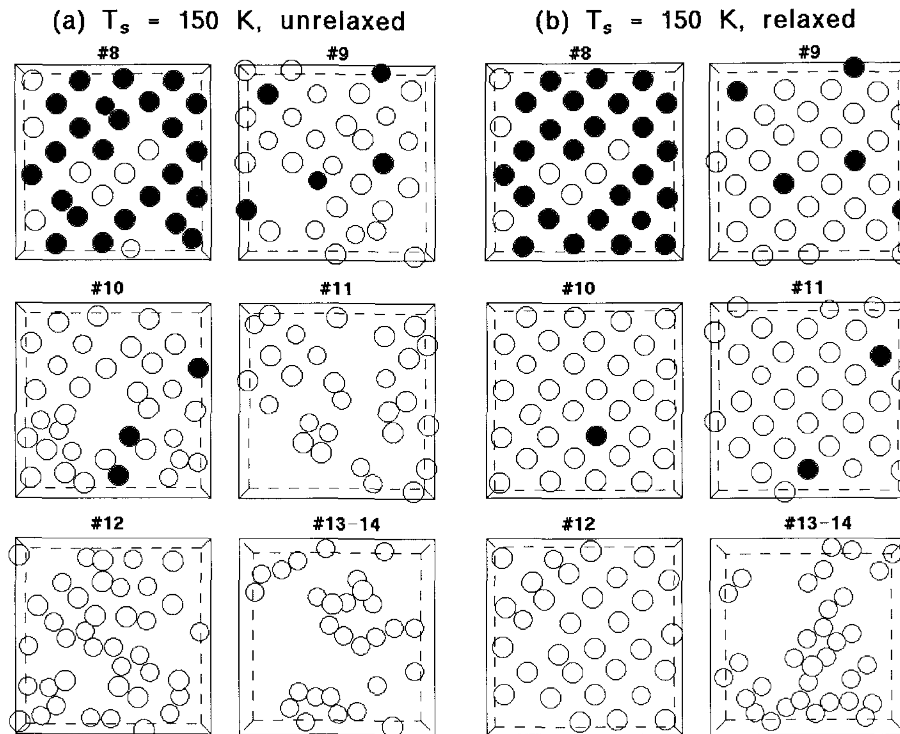

FIG. 3. Homoepitaxy of Si on Si(100) for a substrate temperature of 150 K (a) before and (b) after annealing at 1500 K. Black circles: original substrate; white circles: deposited atoms. Layer labeled #8 is the top layer of the original substrate.

We have also carried out high-temperature depositions. As can be seen in Fig. 4(a), for T_s = 800 K, the preannealed film orders much better than its 150 K counterpart: more energy is available for the incoming atoms, which favors diffusion through the large potential barriers at the surface of covalent semiconductors (exactly the opposite phenomenon takes place at *metallic* surfaces).[20] The importance of diffusion processes can in fact be inferred from the presence of atoms from the initial surface (layer #8) in the topmost layers of the film. Annealing causes most of the defects to disappear, as shown in Fig. 4(b): except at its surface, the film is totally epitaxial.

Further increase in T_s, now, results in serious degradation of the films. At 1500 K, Fig. 5(a), disorder prevails, even for the deepest layers. As we approach fusion, the atoms get more and more energetic and induce a large number of defects. Dynamic processes take place at a very high rate, with atoms from the original surface undergoing extensive diffusion. Figure 5(b) shows that annealing improves the situation, though not satisfactorily. The system is simply too close to melting (i.e., in a state of "premelting") to allow for proper equilibration of the surface. Indeed, in this case, the temperature of the deposited layers increased to about 1900 K, which is slightly above the melting temperature of Stillinger–Weber silicon, namely 1691 K.[32] (Because of the presence of the two fixed layers at the bottom of the substrate, however, we expect the melting temperature to be slightly higher in our model.) In the annealing phase, on the other hand, the temperature was well maintained at 1500 K, but the "damages" were too extensive for the system to recover completely. The growth of this film, in fact, proceeds in a way that is approaching that of the 1800 K deposit, Fig. 6, in which case we found it impossible to grow an epitaxial film: the system effectively melts, though some traces of crystallinity, probably due to the fixed layers, are still visible. (Note that the sequence of layers in Fig. 6 starts at #5, i.e., deep inside the initial substrate; considerable diffusion has therefore taken place.) A substrate temperature of 800–1000 K thus appears to be optimum for epitaxial growth in this model.

C. $Si_{0.5}Ge_{0.5}$ on Si(100)2 × 1

As in the case of homoepitaxy, the growth of $Si_{0.5}Ge_{0.5}$ on a low-temperature substrate proceeds in a disorderly manner, as shown in Fig. 7. Since Si and Ge atoms are created at random with equal probability, an essentially uniform distribution of the two types is observed, and no chemical order is visible. There is also very little interdiffusion at the interface level, owing to the low mobility of substrate atoms at these temperatures. One also notes the presence of large voids in the structure, even in the first deposited layer. In contrast to the case of pure Si, finally, annealing does not significantly improve the order, nor does it appreciably increase the importance of diffusion processes.

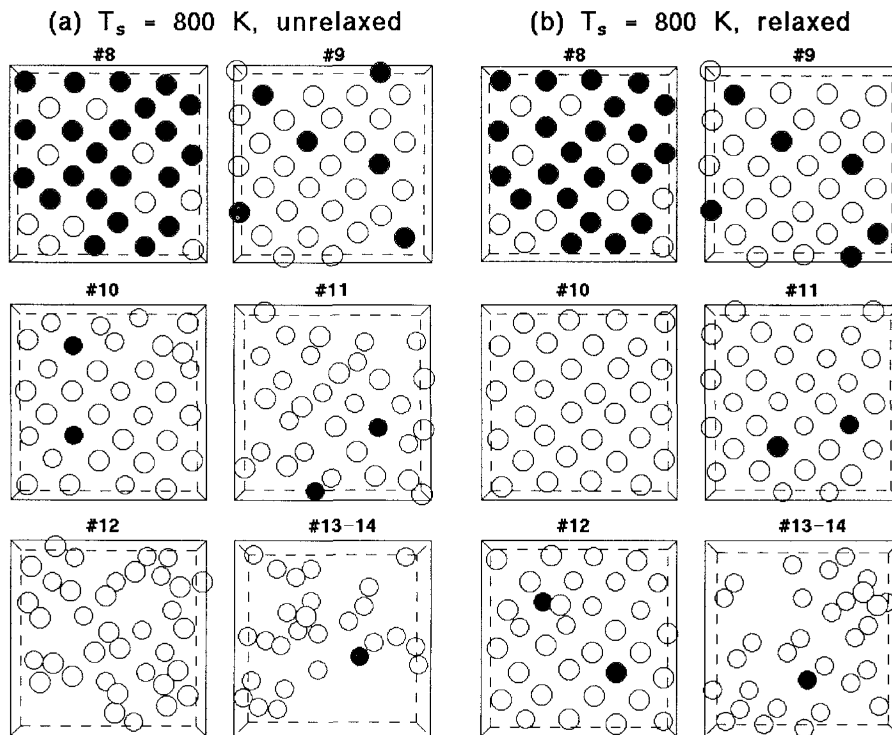

FIG. 4. Same as Fig. 3, but at T_s = 800 K: (a) before and (b) after annealing.

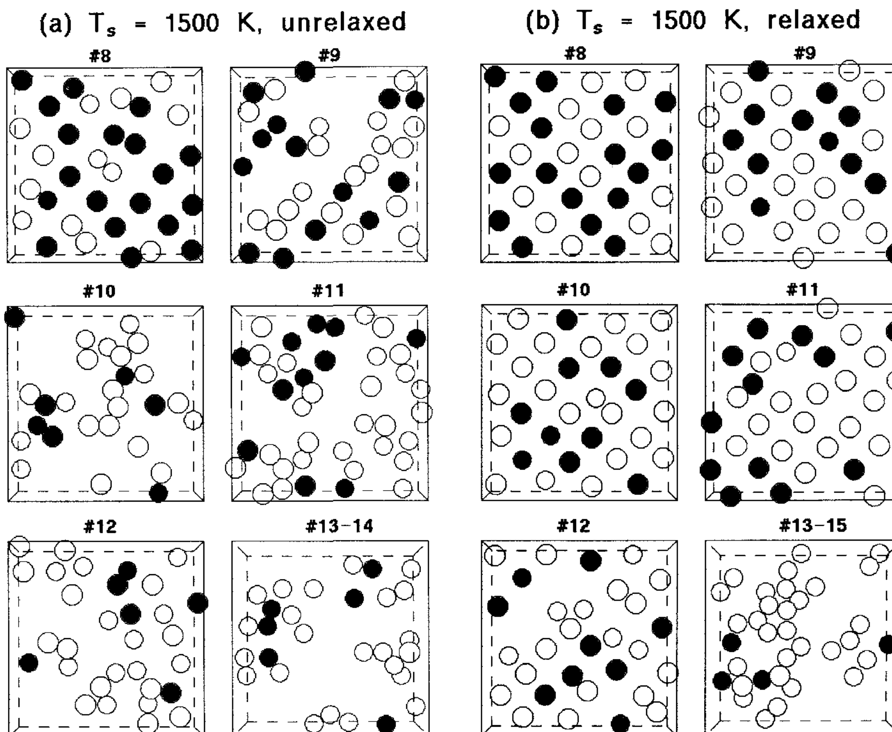

FIG. 5. Same as Fig. 3, but at T_s = 1500 K: (a) before and (b) after annealing.

At high substrate temperature, T_s = 1000 K, Fig. 8, on the other hand, growth is much more epitaxial. We have tried many experiments at different temperatures, and 1000 K appears to give optimum results. In the preannealed state, substantial disorder is present, but signs of crystallinity are omnipresent up to layer #11. The initial surface has recovered its bulk structure. Naturally, more diffusion takes place, but still no chemical order is found. High-temperature annealing now results in considerable improvement of the topological

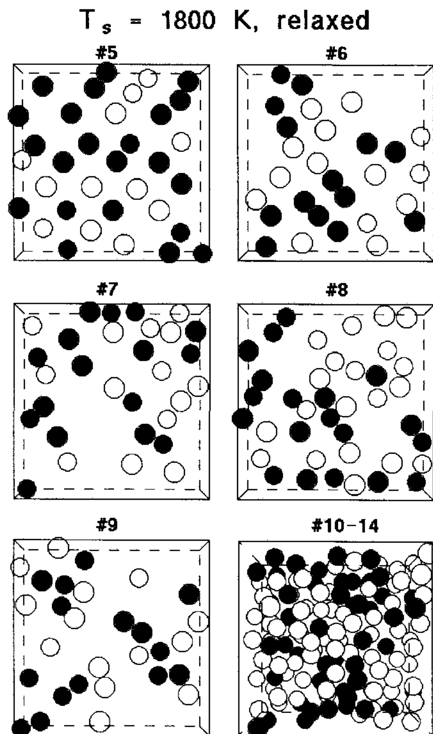

FIG. 6. Same as Fig. 3, but at T_s = 1800 K, after annealing; note that the sequence of layers starts at #5 (top left).

order, which proceeds by the removal of several defects. The heat treatment, again, does not appear to increase interdiffusion, which, we therefore conclude, takes place primarily during growth. Thus, in this case, epitaxy is complete for four out of five adlayers.

It seems that the incorporation of Ge improves the quality of the films when grown at high temperature, while the opposite is true at low temperature. This can be seen more clearly in Fig. 9, where we compare the first two adlayers, in addition to the original surface, for the $Si_{0.5}Ge_{0.5}$ system with the corresponding ones for pure Si deposited under the same conditions, and in both cases *before* annealing. Evidently, $Si_{0.5}Ge_{0.5}$ has "more crystallinity" than pure Si. It is not clear what this effect is due to, and may reflect some delicate balance among various factors in our model, such as mobility, size, and temperature. We note here that the simulations were performed under constant volume; i.e., the lateral dimensions of the system are fixed. Since Ge atoms are larger than Si atoms, this leads to an increase in pressure and, therefore, should result in a *more disordered* structure. Thus, kinematic and activated processes *during* growth play a determinant role in the formation of the equilibrium structure, as has indeed been established experimentally.[5]

D. Ge on Si(100)2 × 1

Finally, we investigate the structure of deposits of Ge on Si(100). At low temperature, we obtain results

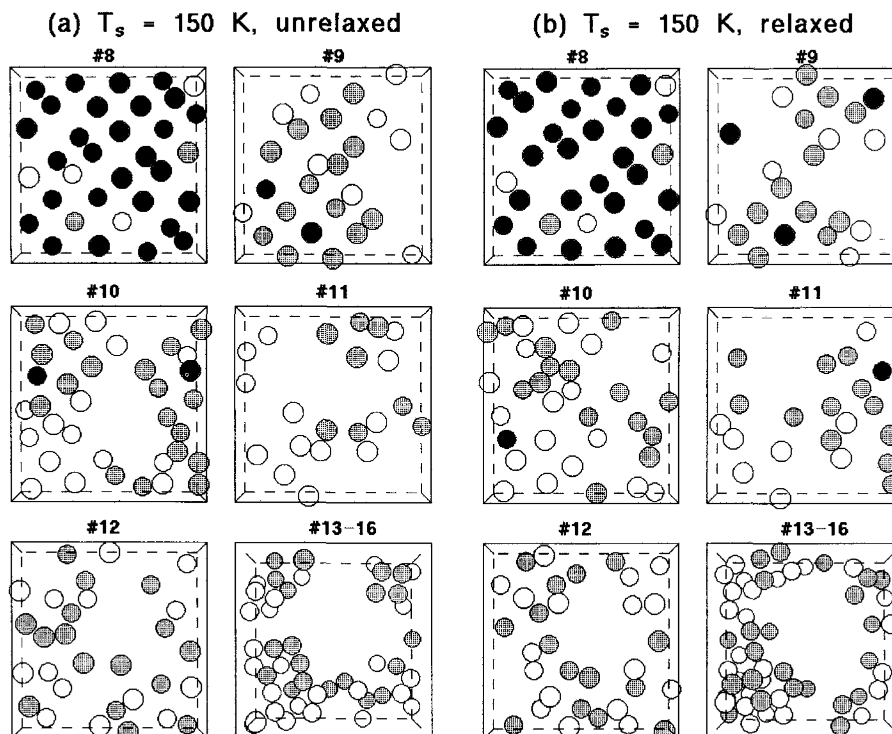

FIG. 7. Heteroepitaxy of $Si_{0.5}Ge_{0.5}$ on Si(100) for a substrate temperature of 150 K: (a) before and (b) after annealing at 1500 K. Black circles: original Si substrate; white circles: deposited Si atoms; grey circles: deposited Ge atoms.

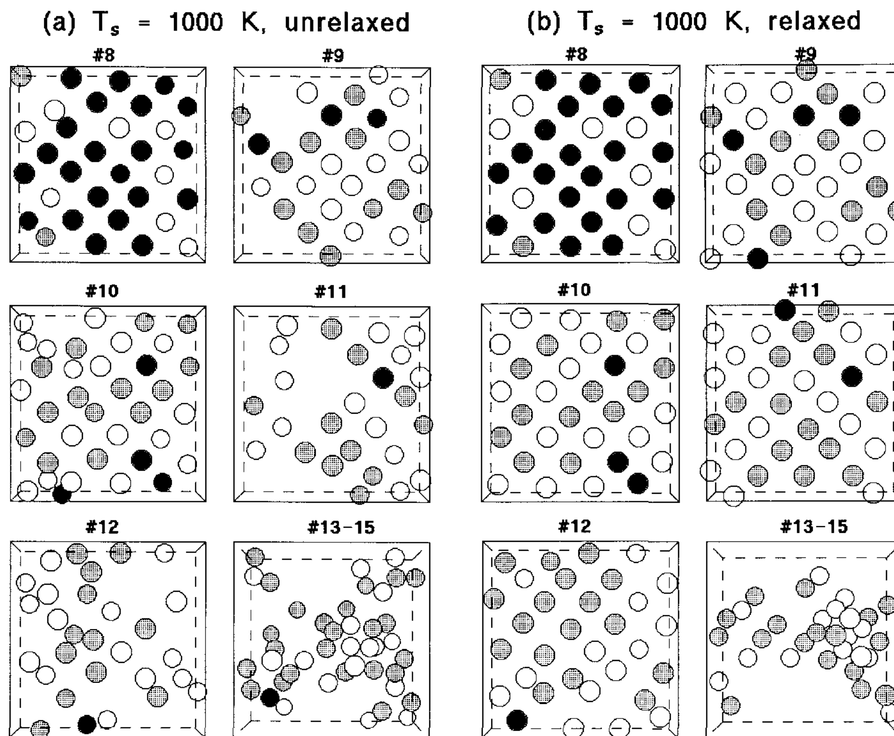

FIG. 8. Same as Fig. 7, but at T_s = 1000 K: (a) before and (b) after annealing.

in all points equivalent to the previous case: all deposited layers are topologically disordered, and very little diffusion takes place. This is shown in Fig. 10.

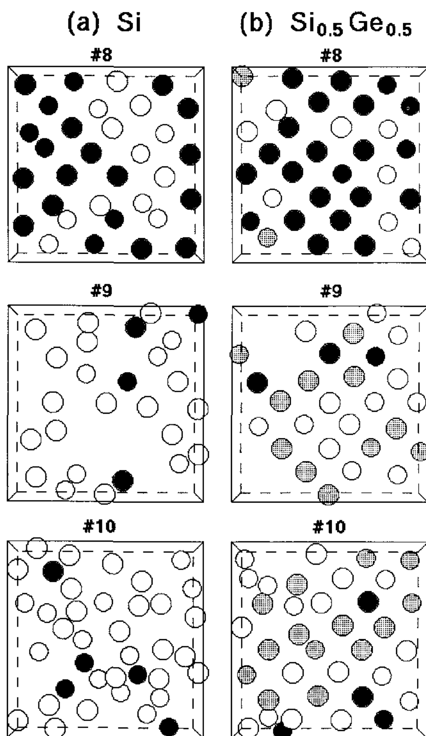

FIG. 9. Comparison between (a) Si and (b) $Si_{0.5}Ge_{0.5}$ deposits grown under the same conditions at T_s = 1000 K, before annealing.

High-temperature annealing has essentially no effect, except for a small reordering at the interface level. Thus, while the interface is sharp, the deposited layers have poor crystallinity.

At a substrate temperature of 1000 K, Fig. 11, the topological order improves considerably, and a large interdiffusion of the two species at the interface level is observed. Si atoms from the substrate are "knocked off" by incident Ge atoms, which causes the interface to broaden, spreading over four monolayers (≈6 Å) (the sequence of layers in Fig. 11 starts at #7, i.e., one layer below the original surface). Thus the interface is chemically rough, but topologically smooth.

Growth occurs epitaxially in its initial stage, then crosses over to the formation of islands and clusters. This can be seen in Fig. 11, but is shown more clearly in Fig. 12. High-temperature heat treatment results in improved topological order for the first few deposited layers only. The topmost layers remain disordered because of the important lattice mismatch which the fixed volume can no longer accommodate. Germanium has a lattice constant 4% higher than silicon; thus Ge atoms cannot fit in the Si lattice without dramatically increasing the pressure parallel to the layers. Since the [100] direction is free of constraints, Ge atoms compensate by moving in this direction. The sample is therefore thicker, with more disordered layers than pure Si, and growth proceeds by the formation of clusters. This is reminiscent of the growth-mode proposed by Stranski and Krastanow.[30] It is, however, not possible, because of finite-size effects,

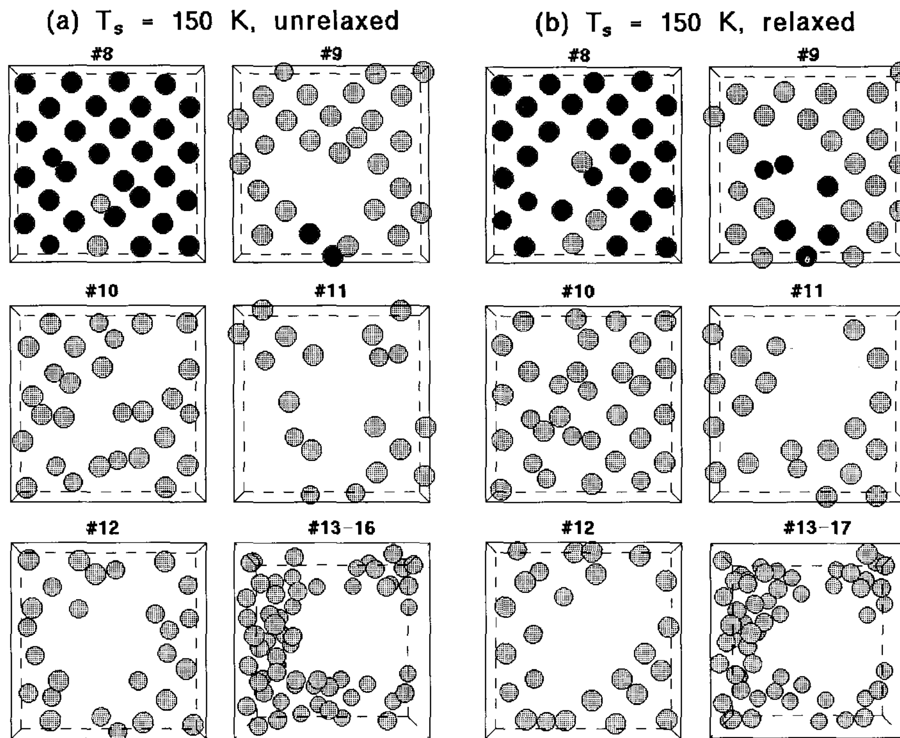

FIG. 10. Heteroepitaxy of Ge on Si(100) for a substrate temperature of 150 K (a) before and (b) after annealing at 1500 K. Black circles: original Si substrate; grey circles: deposited Ge atoms.

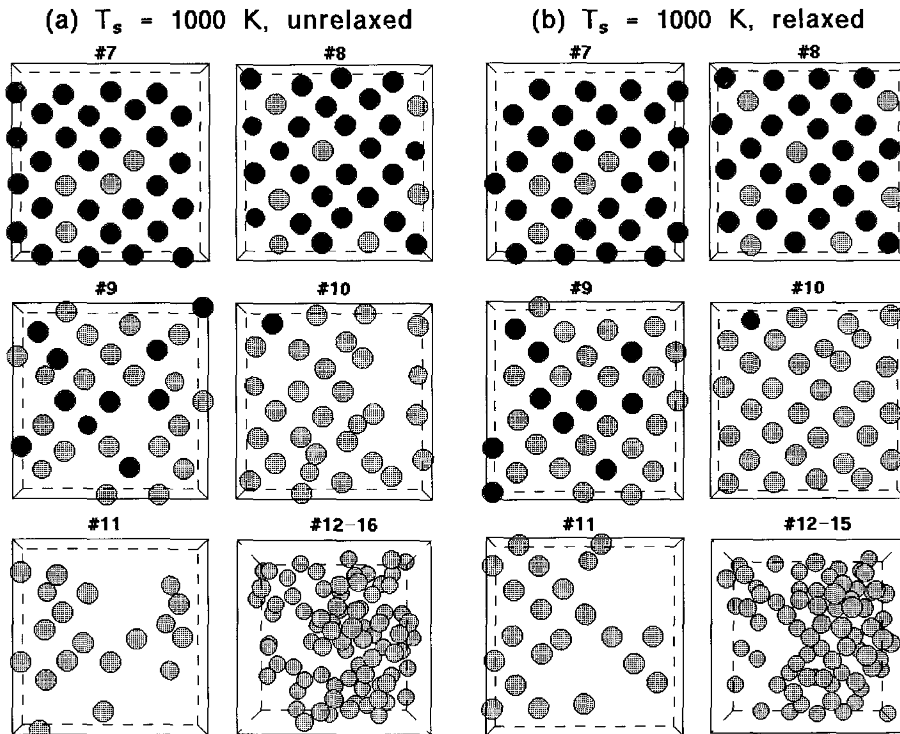

FIG. 11. Same as Fig. 10, but at T_s = 1000 K; note that the sequence of layers starts at #7 (top left): (a) before and (b) after annealing.

to ascertain that growth is indeed Stranski–Krastanow: even though some crystalline features can be identified in the cluster of layers 12–15 (Fig. 11), the presence of such a structure may simply be indicative of an atomically rough surface. Our results are nevertheless in excellent agreement with recent experimental[4,7,8] and

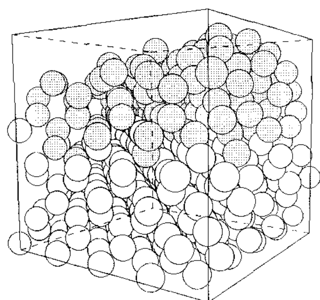

FIG. 12. The pure Ge sample after annealing, corresponding to Fig. 11(b), showing the formation of islands.

theoretical[14] studies which find that epitaxial growth takes place for the first three monolayers only. Layer-by-layer growth ensures that the strain energy resulting from surface dimerization is minimized. When some critical thickness is reached, however, the strain associated with the Si/Ge lattice mismatch becomes dominant, and the system then relaxes its energy by crossing over to growth *à la* Stranski–Krastanow.

IV. SUMMARY AND CONCLUSIONS

We have used the technique of molecular dynamics to investigate the growth of $Si_{1-x}Ge_x$ on Si(100) in a way appropriate to the physical process of molecular-beam epitaxy, i.e., by sequential deposition of energetic atoms on the surface. The energy was modeled in terms of potentials of the Stillinger–Weber form; in particular, for mixed interactions, the parameters were determined by interpolating between the pure substances using standard combining rules. As expected, the model reproduces very well the 2 × 1 reconstruction of the surface. All deposits were done on this reconstructed surface.

Our simulations show that at low substrate temperatures, the deposited layers exhibit considerable disorder, and that little interdiffusion takes place at the interface level. The disorder is such that high-temperature annealing has little effect on these samples. At high temperatures, on the other hand, we observe good-quality epitaxial growth for almost all deposits. In all cases, subsequent heat treatment improves the topological order even more, resulting in a very small concentration of defects. Further, under identical conditions, it appears that the presence of Ge improves the crystallinity of the films. For high-temperature growth, large diffusive motion is found to occur at the interface which, in the case of pure Ge, results in a rough interface. In the latter, we also observe growth that proceeds in a way consistent with that proposed by Stranski and Krastanow.

The present study constitutes a first step toward the simulation of the growth of mixed semiconductor films. This could easily be extended to the study of other systems, such as III-V compounds. Several improvements to the model can, however, be envisaged. The potentials, in particular, could be optimized in a more systematic way. In addition, the spatial constraints resulting from the use of a fixed volume could also be relaxed. This will be the object of further investigations.

ACKNOWLEDGMENTS

This work was supported by the Natural Science and Engineering Research Council (NSERC) of Canada, as well as by the Fonds pour la formation de chercheurs et l'aide à la recherche and Actions structurantes programs of the Government of Québec. Part of the calculations reported here were performed on the Cray Research Inc. X-MP supercomputer at the Ontario Center for Large-Scale Computation. One of us (S.E.) is grateful to NSERC for a postgraduate fellowship.

REFERENCES

1. See, for instance, R. People, IEEE, J. Quantum Electron. **QE-22** 1696 (1986); R. People, J. C. Bean, D. V. Lang, A. M. Sergent, H. L. Störmer, K. W. Wecht, R. T. Lynch, and K. Baldwin, Appl. Phys. Lett. **45**, 1231 (1984); R. People, J. C. Bean, and D. V. Lang, J. Vac. Sci. Technol. **A3**, 3, 846 (1985).
2. See, for instance, various articles in *Deposition Processes,* Parts I and II, MRS Bull. **XIII**, No. 11 and 12, November 1988.
3. M. A. Herman and H. Sitter, in *Molecular-Beam Epitaxy: Fundamentals and Current Status,* edited by M. B. Panish, Springer Series in Materials Science (Springer, Berlin, 1989), Vol. 7; see also various articles in *The Technology and Physics of Molecular-Beam Epitaxy,* edited by E. H. C. Parker (Plenum Press, New York, 1985).
4. H. Jorke and H. J. Herzog, in *Proc. 1st Int. Symp. on Silicon Molecular Beam Epitaxy,* edited by J. C. Bean (Electrochemical Soc., Pennington, NJ, 1985), p. 352; G. Abstreiter, H. Brugger, T. Wolf, H. Jorke, and H. J. Herzog, Phys. Rev. Lett. **54**, 2441 (1985); H. Jorke, H. J. Herzog, and H. Kibbel, Phys. Rev. B **40**, 2005 (1989).
5. F. K. LeGoues, V. P. Kesan, S. S. Iyer, J. Tersoff, and R. Tromp, Phys. Rev. Lett. **64**, 2038 (1990); F. K. LeGoues, M. Copel, and R. Tromp, Phys. Rev. Lett. **63**, 1826 (1989); F. K. LeGoues, V. P. Kesan, and S. S. Iyer, Phys. Rev. Lett. **64**, 408 (1990).
6. J. C. Woicik, C. E. Bouldin, M. I. Bell, J. O. Cross, D. J. Tweet, B. D. Swanson, T. M. Zhang, L. B. Sorensen, C. A. King, J. L. Hoyt, P. Pianetta, and J. F. Gibbons, Phys. Rev. B **43**, 2419 (1991).
7. A. A. Williams, J. M. C. Thornton, J. E. Macdonald, R. G. van Silfhout, J. F. van der Veen, M. S. Finney, A. D. Johnson, and C. Norris, Phys. Rev. B **43**, 5001 (1991).
8. D. J. Eaglesham and M. Cerullo, Phys. Rev. Lett. **64**, 1943 (1990); D. J. Eaglesham, H-J. Gossmann, and M. Cerullo, Phys. Rev. Lett. **63**, 1227 (1990).
9. Y-W. Mo, D. E. Savage, B. S. Swartzentruber, and M. G. Lagally, Phys. Rev. Lett. **65**, 1020 (1990).
10. E. Vlieg, A. W. Denier van der Gon, J. F. van der Veen, J. E. Mcdonald, and C. Norris, Phys. Rev. Lett. **61**, 2241 (1988).
11. T. P. Pearsall, J. M. Vandenberg, R. Hull, and J. M. Bonar, Phys. Rev. Lett. **63**, 2104 (1989).
12. H. Neddermeyer and S. Tosch, Phys. Rev. B **38**, 5784 (1988).
13. A. Qteish and E. Molinari, Phys. Rev. B **42**, 7090 (1990).
14. J. Tersoff, Phys. Rev. B **43**, 9377 (1991).

15. S. de Gironcoli, P. Gianozzi, and S. Baroni, Phys. Rev. Lett. **66**, 2116 (1991).
16. B. Koiller and M. O. Robbins, Phys. Rev. B **40**, 12554 (1989).
17. See, for instance, numerous articles in *Atomic-Scale Calculations in Materials Science,* edited by J. Tersoff, D. Vanderbilt, and V. Vitek (Mater. Res. Soc. Symp. Proc. **141**, Pittsburgh, PA, 1989).
18. E. T. Gawlinski and J. D. Gunton, Phys. Rev. B **36**, 4774 (1987).
19. M. Schneider, I. K. Schuller, and A. Rahman, Phys. Rev. B **36**, 1340 (1987).
20. I. K. Schuller, in Ref. 2, p. 23.
21. I. Kwon, R. Biswas, G. S. Grest, and C. M. Soukoulis, Phys. Rev. B **41**, 3678 (1990).
22. W. D. Luedtke and Uzi Landman, Phys. Rev. B **40**, 11733 (1989); U. Landman, W. D. Luedtke, M. W. Ribarsky, R. N. Barnett, and C. L. Cleveland, Phys. Rev. B **37**, 4637 (1988); W. D. Luedtke, U. Landman, M. W. Ribarsky, R. N. Barnett, and C. L. Cleveland, Phys. Rev. B **37**, 4647 (1988).
23. B. W. Dodson, Phys. Rev. B **36**, 1068 (1987).
24. B. J. Garrison, M. T. Miller, and D. W. Brenner, in Ref. 17, p. 419.
25. K. E. Khor and S. Das Sarma, Phys. Rev. B **36**, 7733 (1987).
26. J. Lampinen, R. M. Nieminen, and K. Kaski, Surf. Sci. **203**, 201 (1988).
27. G. H. Gilmer and A. F. Bakker, in *Computer-Aided Innovation of New Materials,* edited by M. Doyama, T. Suzuki, J. Kihara, and R. Yamamoto (Elsevier, Amsterdam).
28. Recent studies of bulk Si–Ge alloys include A. Qteish and R. Resta, Phys. Rev. B **37**, 1308 (1988); *ibid.,* 6983 (1988); M. I. Alonso and K. Winer, Phys. Rev. B **39**, 10056 (1989).
29. A preliminary account of this work has been given in S. Ethier and L. J. Lewis, in *Evolution of Thin Film and Surface Microstructure,* edited by C. V. Thompson, J. Y. Tsao, and D. J. Srolovitz (Mater. Res. Soc. Symp. Proc. **202**, Pittsburgh, PA, 1991), p. 371.
30. I. N. Stranski and Von L. Krastanow, Akad. Wiss. Lit. Mainz Math.-Natur. Kl. IIb **146**, 797 (1939).
31. F. H. Stillinger and T. A. Weber, Phys. Rev. B **31**, 5262 (1985).
32. J. Q. Broughton and X. P. Li, Phys. Rev. B **35**, 9120 (1987).
33. K. E. Khor and S. Das Sarma, Phys. Rev. B **38**, 3318 (1988).
34. J. Tersoff, Phys. Rev. Lett. **56**, 632 (1986).
35. R. Biswas and D. R. Hamann, Phys. Rev. Lett. **55**, 2001 (1985).
36. E. R. Cowley, Phys. Rev. Lett. **60**, 2379 (1988).
37. R. Car and M. Parrinello, Phys. Rev. Lett. **55**, 2471 (1985). Pertinent applications of the method include S. Ihara, S. L. Ho, T. Uda, and M. Hirao, Phys. Rev. Lett. **65**, 1909 (1990); F. Ancilotto, W. Andreoni, A. Selloni, R. Car, and M. Parrinello, Phys. Rev. Lett. **65**, 3148 (1990); M. Needels, M. C. Payne, and J. D. Joannopoulos, Phys. Rev. Lett. **58**, 1765 (1987).
38. T. Ito, K. E. Khor, and S. Das Sarma, Phys. Rev. B **40**, 9715 (1989).
39. K. E. Khor and S. Das Sarma, Phys. Rev. B **43**, 9992 (1991).
40. K. Ding and H. C. Andersen, Phys. Rev. B **34**, 6987 (1986).
41. M. P. Allen and D. J. Tildesley, *Computer Simulation of Liquids* (Clarendon Press, Oxford, 1987).
42. J. P. Dismukes, L. Ekstrom, and R. J. Paff, J. Phys. Chem. **68**, 3021 (1964).
43. C. W. Gear, *Numerical Initial Value Problems in Ordinary Differential Equations* (Prentice-Hall, Englewood Cliffs, NJ, 1971), Chap. 9.
44. L. J. Lewis and M. L. Klein, in *Dynamical Properties of Solids,* edited by G. K. Horton and A. A. Maradudin (North-Holland, Amsterdam, 1990), Vol. 6, Chap. 7, p. 383.
45. J. Y. Tsao, E. Chason, U. Koehler, and R. Hamers, Phys. Rev. B **40**, 11951 (1989).